

The transient and frequency response analysis using the multi-level system condensation in the large-scaled structural dynamic problem

Sungmin Baek and Maenghyo Cho*

*WCU Multiscale Mechanical Design Division, School of Mechanical and Aerospace Engineering,
Seoul National University, Seoul, Korea*

(Received April 22, 2010, Accepted February 22, 2011)

Abstract. In large-scale problem, a huge size of computational resources is needed for a reliable solution which represents the detailed description of dynamic behavior. Recently, eigenvalue reduction schemes have been considered as important technique to resolve computational resource problems. In addition, the efforts to advance an efficiency of reduction scheme leads to the development of the multi-level system condensation (MLSC) which is initially based on the two-level condensation scheme (TLCS). This scheme was proposed for approximating the lower eigenmodes which represent the global behavior of the structures through the element-level energy estimation. The MLSC combines the multi-level sub-structuring scheme with the previous TLCS for enhancement of efficiency which is related to computer memory and computing time. The present study focuses on the implementation of the MLSC on the direct time response analysis and the frequency response analysis of structural dynamic problems. For the transient time response analysis, the MLSC is combined with the Newmark's time integration scheme. Numerical examples demonstrate the efficiency of the proposed method.

Keywords: structural dynamic system; system condensation; reduced system method; transient time integration; sub-structuring scheme; two-level condensation scheme.

1. Introduction

In spite of enormous advance in digital computer capability, more and more large-scaled detailed numerical models are constructed for the detailed prediction of the system behavior. To satisfy this requirement, it is efficient to introduce modal reduction. In structural dynamic analysis, the model reduction techniques are classified into two-category, degree-of-freedom based reduction (DBR) and mode-based reduction (MBR).

The representative method of MBR is Component Mode Synthesis (CMS) method. It was initially developed by Craig and Bampton (1960) and have been revitalized in recent years. Now, it has been lead by the Automated Multi-Level Sub-structuring method (Benninghof and Lehoucq 2004). The MBR has an advantage in its convenient construction procedure. However, the MBR has a truncation error which is related to high frequency modes.

On the other hand, the DBR includes the effects of high frequency modes within condensation

*Corresponding author, Professor, E-mail: mhcho@snu.ac.kr

procedure. Moreover, the DBR maintains the degrees of freedom (DOFs) in the physical domain after completing the reduction procedure, contrary to MBR which transforms DOFs into generalized coordinates. Since static condensation (Guyan 1965), various DBR techniques have been developed in order to circumvent a limitation on digital computer resources (O'callahan 1989, Friswell *et al.* 1995, Kim and Kang 2001). The original system is reduced into smaller system through the transformation matrix between the primary degrees of freedom (PDOFs) and the secondary degrees of freedom (SDOFs) through the condensation procedures with assuring the solution accuracy within the allowable error bounds. In fact, each condensation techniques have different scale of the transformation error. Hence, it is required to select a reduction method which satisfies allowable error tolerance. In this study, we adopted the IIRS techniques in the condensation process because the IIRS technique is the optimized method to reduce DOFs transformation error (Friswell *et al.* 1998).

Basically, system condensation techniques have another critical issue that is the selection of PDOFs. It is directly related with the solution accuracy and convergence of the reduced system and dominant effect on the reliability of the reduced system. In addition, the selection of the PDOFs has a similarity with that of sensor locations in damage detection problems. Hence, various studies have been performed for appropriate PDOFs selection scheme. In general, the Sequential Elimination method (SEM) (Henshell and Ong 1975, Shah and Raymund 1982) shows the most reliable selection of PDOFs and the predictions of lower mode eigenvalues are very reliable. However, it takes excessive computing time for selecting the PDOFs because it eliminates only a single DOF in each iteration step. In order to reduce this trouble of the SEM, the Two-Level Condensation scheme (TLCS) was proposed for eigenvalue problems (Cho and Kim 2004).

Recently, the two-level condensation scheme (TLCS) which combined with sub-structuring scheme was proposed. (Cho and Kim 2004, Kim and Cho 2006, 2007) The previous study shows remarkable advances in the practical application of the system condensation on the large-scaled structural dynamic problem. However, the previous TLCS combined with sub-structuring method has a trouble in the reduction of interface region between sub-structures. When original system divided into a huge number of substructures, size of interface region becomes important part of system information and the effect of interface DOFs cannot be neglected. The size of interface region behaves as the bottleneck in the computational memory in the reduction process.

In the present study, we present the multi-level system condensation (MLSC) which is initially based on the TLCS, Iterated IRS techniques. The proposed reduction method can dramatically reduce the final size of the reduced system and improve its accuracy. We apply the MLSC to transient time response analysis and frequency response analysis. The efficiency of the proposed method is demonstrated through the numerical examples.

2. The multi-level system condensation

2.1 Formulation of the multi-level system condensation

A general mathematical derivation of equation of motion is given as

$$\mathbf{M}\ddot{\mathbf{x}} + \mathbf{C}\dot{\mathbf{x}} + \mathbf{K}\mathbf{x} = \mathbf{f}(t) \quad (1)$$

where \mathbf{M} , \mathbf{C} and \mathbf{K} are mass, damping and stiffness matrices, respectively. $\mathbf{f}(t)$ is the applied force and \mathbf{x} , $\dot{\mathbf{x}}$ and $\ddot{\mathbf{x}}$ are the structural displacement, velocity and acceleration vector. In the undamped

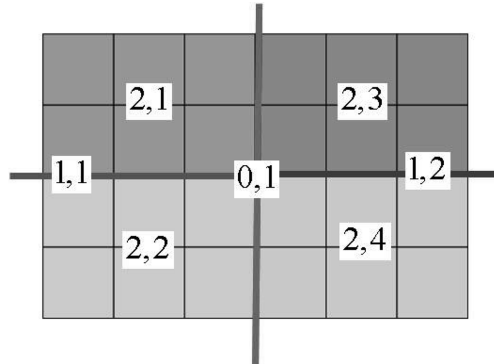


Fig. 1 Configuration of the simple plate example

free vibration problem, the trial solution, $\mathbf{x}(t) = \mathbf{x}e^{i\omega t}$ leads to the generalized eigenvalue problem which is represented as

$$\mathbf{K}\mathbf{x} = \lambda\mathbf{M}\mathbf{x} \tag{2}$$

where \mathbf{K} and \mathbf{M} are stiffness and mass matrix. The original system divided into several sub-structures through hierarchical graph partitioning procedure. In this section, four sub-structure case through two level graph partitioning procedure which is presented in Fig. 1 is presented. The governing Eq. (2) is divided and rearranged as shown in Eq. (3a) and (3b) and rearranged displacement field is presented in Eq. (3c). The symbol (i, j) means j th domain which is partitioned at the i th level. The highest level means interior part of each substructures and lower level means interface region between adjacent sub-structures.

$$\mathbf{K} = \begin{bmatrix} \mathbf{K}_{(2,1)} & 0 & \mathbf{K}_{(2,1)(1,1)} & 0 & 0 & 0 & \mathbf{K}_{(2,1)(0,1)} \\ & \mathbf{K}_{(2,2)} & \mathbf{K}_{(2,2)(1,1)} & 0 & 0 & 0 & \mathbf{K}_{(2,2)(0,1)} \\ & & \mathbf{K}_{(1,1)} & 0 & 0 & 0 & \mathbf{K}_{(1,1)(0,1)} \\ & & & \mathbf{K}_{(2,3)} & 0 & \mathbf{K}_{(2,3)(0,1)} & \mathbf{K}_{(2,3)(0,1)} \\ & & & & \mathbf{K}_{(2,4)} & \mathbf{K}_{(2,4)(0,1)} & \mathbf{K}_{(2,4)(0,1)} \\ & & \text{symm.} & & & \mathbf{K}_{(1,2)} & \mathbf{K}_{(1,2)(0,1)} \\ & & & & & & \mathbf{K}_{(0,1)} \end{bmatrix} \tag{3a}$$

$$\mathbf{M} = \begin{bmatrix} \mathbf{M}_{(2,1)} & 0 & \mathbf{M}_{(2,1)(1,1)} & 0 & 0 & 0 & \mathbf{M}_{(2,1)(0,1)} \\ & \mathbf{M}_{(2,2)} & \mathbf{M}_{(2,2)(1,1)} & 0 & 0 & 0 & \mathbf{M}_{(2,2)(0,1)} \\ & & \mathbf{M}_{(1,1)} & 0 & 0 & 0 & \mathbf{M}_{(1,1)(0,1)} \\ & & & \mathbf{M}_{(2,3)} & 0 & \mathbf{M}_{(2,3)(0,1)} & \mathbf{M}_{(2,3)(0,1)} \\ & & & & \mathbf{M}_{(2,4)} & \mathbf{M}_{(2,4)(0,1)} & \mathbf{M}_{(2,4)(0,1)} \\ & & \text{symm.} & & & \mathbf{M}_{(1,2)} & \mathbf{M}_{(1,2)(0,1)} \\ & & & & & & \mathbf{M}_{(0,1)} \end{bmatrix} \tag{3b}$$

$$\mathbf{x} = [\mathbf{x}_{(2,1)} \quad \mathbf{x}_{(2,2)} \quad \mathbf{x}_{(1,1)} \quad \mathbf{x}_{(2,3)} \quad \mathbf{x}_{(2,4)} \quad \mathbf{x}_{(1,2)} \quad \mathbf{x}_{(0,1)}]^T \quad (3c)$$

After transformation of each sub-structure through the block Gaussian eliminator given in Eq. (5), each domain has an independency to each other as described in Eq. (7a) and (7b). In the multi-level sub-structuring case, the block Gaussian eliminator is separated according to the graph partitioning level as shown in Eq. (6a) and (6b), and \mathbf{U}_i means i th level eliminator. Due to the separation of the eliminator, the factorization of each domain can be performed independently to other domains.

$$\mathbf{U} = \mathbf{U}_0 \mathbf{U}_1 \quad (4)$$

where

$$\mathbf{U}_0 = \begin{bmatrix} \mathbf{I}_{(2,1)} & 0 & -\mathbf{K}_{(2,1)}^{-1} \mathbf{K}_{(2,1)(1,1)} & 0 & 0 & 0 & -\mathbf{K}_{(2,1)}^{-1} \mathbf{K}_{(2,1)(1,0)} \\ 0 & \mathbf{I}_{(2,2)} & -\mathbf{K}_{(2,2)}^{-1} \mathbf{K}_{(2,2)(1,1)} & 0 & 0 & 0 & -\mathbf{K}_{(2,2)}^{-1} \mathbf{K}_{(2,2)(1,0)} \\ 0 & 0 & \mathbf{I}_{(1,1)} & 0 & 0 & 0 & 0 \\ 0 & 0 & 0 & \mathbf{I}_{(2,3)} & 0 & -\mathbf{K}_{(2,1)}^{-1} \mathbf{K}_{(2,3)(1,2)} & -\mathbf{K}_{(2,1)}^{-1} \mathbf{K}_{(2,3)(1,0)} \\ 0 & 0 & 0 & 0 & \mathbf{I}_{(2,4)} & -\mathbf{K}_{(2,1)}^{-1} \mathbf{K}_{(2,4)(1,2)} & -\mathbf{K}_{(2,1)}^{-1} \mathbf{K}_{(2,4)(1,0)} \\ 0 & 0 & 0 & 0 & 0 & \mathbf{I}_{(1,2)} & 0 \\ 0 & 0 & 0 & 0 & 0 & 0 & \mathbf{I}_{(0,1)} \end{bmatrix} \quad (5a)$$

$$\mathbf{U}_1 = \begin{bmatrix} \mathbf{I}_{(2,1)} & 0 & 0 & 0 & 0 & 0 & 0 \\ 0 & \mathbf{I}_{(2,2)} & 0 & 0 & 0 & 0 & 0 \\ 0 & 0 & \mathbf{I}_{(1,1)} & 0 & 0 & 0 & -\bar{\mathbf{K}}_{(1,1)}^{-1} \bar{\mathbf{K}}_{(1,1)(0,1)} \\ 0 & 0 & 0 & \mathbf{I}_{(2,3)} & 0 & 0 & 0 \\ 0 & 0 & 0 & 0 & \mathbf{I}_{(2,4)} & 0 & 0 \\ 0 & 0 & 0 & 0 & 0 & \mathbf{I}_{(1,2)} & -\bar{\mathbf{K}}_{(1,2)}^{-1} \bar{\mathbf{K}}_{(1,2)(0,1)} \\ 0 & 0 & 0 & 0 & 0 & 0 & \mathbf{I}_{(0,1)} \end{bmatrix} \quad (5b)$$

Due to the factorization of Eq. (5), stiffness and mass matrices are decomposed into the block-diagonalized form which is shown below

$$\bar{\mathbf{K}} = \mathbf{U}^T \mathbf{K} \mathbf{U} = \text{diag}[\bar{\mathbf{K}}_{(2,1)} \quad \bar{\mathbf{K}}_{(2,2)} \quad \bar{\mathbf{K}}_{(1,1)} \quad \bar{\mathbf{K}}_{(2,3)} \quad \bar{\mathbf{K}}_{(2,4)} \quad \bar{\mathbf{K}}_{(1,2)} \quad \bar{\mathbf{K}}_{(0,1)}] \quad (6a)$$

$$\bar{\mathbf{M}} = \mathbf{U}^T \mathbf{M} \mathbf{U} = \begin{bmatrix} \bar{\mathbf{M}}_{(2,1)} & 0 & \bar{\mathbf{M}}_{(2,1)(1,1)} & 0 & 0 & 0 & \bar{\mathbf{M}}_{(2,1)(0,1)} \\ & \bar{\mathbf{M}}_{(2,2)} & \bar{\mathbf{M}}_{(2,2)(1,1)} & 0 & 0 & 0 & \bar{\mathbf{M}}_{(2,2)(0,1)} \\ & & \bar{\mathbf{M}}_{(1,1)} & 0 & 0 & 0 & \bar{\mathbf{M}}_{(1,1)(0,1)} \\ & & & \bar{\mathbf{M}}_{(2,3)} & 0 & \bar{\mathbf{M}}_{(2,3)(0,1)} & \bar{\mathbf{M}}_{(2,3)(0,1)} \\ & & & & \bar{\mathbf{M}}_{(2,4)} & \bar{\mathbf{M}}_{(2,4)(0,1)} & \bar{\mathbf{M}}_{(2,4)(0,1)} \\ & & \text{symm.} & & & \bar{\mathbf{M}}_{(1,2)} & \bar{\mathbf{M}}_{(1,2)(0,1)} \\ & & & & & & \bar{\mathbf{M}}_{(0,1)} \end{bmatrix} \quad (6b)$$

The approximated eigenvalue problems of i th level j th sub-domain are constructed with the diagonal parts of the transformed system metrics, Eq. (7a) and (7b). Here, it is assumed that is the effect of off-diagonal parts of mass matrix is less dominant to solution space than diagonal parts.

$$\bar{\mathbf{K}}_{(i,j)}\bar{\mathbf{x}}_{(i,j)} - \lambda\bar{\mathbf{M}}_{(i,j)}\bar{\mathbf{x}}_{(i,j)} = 0 \tag{7}$$

Each decoupled eigenvalue problem of Eq. (7) can be represented as the form divided by primary and secondary DOFs. From the relation between the primary and the secondary DOFs, the transformation matrix can be obtained as $\bar{\mathbf{x}}_{(i,j)} = \mathbf{T}_{(i,j)}\bar{\mathbf{x}}_{(i,j)}^p$ using the IIRS technique (Friswell 1995). The details are confirmed in the reference. The transformation matrix $\mathbf{T}_{(i,j)}$ condenses each decoupled eigenvalue problems of Eq. (8) as below.

$$\bar{\mathbf{K}}_{(i,j)}^R\bar{\mathbf{x}}_{(i,j)}^p - \lambda\bar{\mathbf{M}}_{(i,j)}^R\bar{\mathbf{x}}_{(i,j)}^p \tag{8}$$

where

$$\bar{\mathbf{K}}_{(i,j)}^R = \mathbf{T}_{(i,j)}^T\bar{\mathbf{K}}_{(i,j)}\mathbf{T}_{(i,j)}, \quad \bar{\mathbf{M}}_{(i,j)}^R = \mathbf{T}_{(i,j)}^T\bar{\mathbf{M}}_{(i,j)}\mathbf{T}_{(i,j)} \tag{9}$$

And the final form of transformation matrix is represented as Eq. (10).

$$\mathbf{T} = \text{diag}[\mathbf{T}_{(2,1)} \quad \mathbf{T}_{(2,2)} \quad \mathbf{T}_{(1,1)} \quad \mathbf{T}_{(2,3)} \quad \mathbf{T}_{(2,4)} \quad \mathbf{T}_{(1,2)} \quad \mathbf{T}_{(0,1)}] \tag{10}$$

After assembly of each reduced systems given in Eq. (17), the original governing equation in Eq. (2) is finally condensed into Eq. (19).

$$\bar{\mathbf{K}}^R\bar{\mathbf{x}}^p - \lambda\bar{\mathbf{M}}^R\bar{\mathbf{x}}^p = 0 \tag{11}$$

where

$$\bar{\mathbf{K}}^R = \mathbf{T}^T(\mathbf{U}^T\mathbf{K}\mathbf{U})\mathbf{T} = \text{diag}\mathbf{T} = \text{diag}[\bar{\mathbf{K}}_{(2,1)}^R \quad \bar{\mathbf{K}}_{(2,2)}^R \quad \bar{\mathbf{K}}_{(1,1)}^R \quad \bar{\mathbf{K}}_{(2,3)}^R \quad \bar{\mathbf{K}}_{(2,4)}^R \quad \bar{\mathbf{K}}_{(1,2)}^R \quad \bar{\mathbf{K}}_{(0,1)}^R] \tag{12a}$$

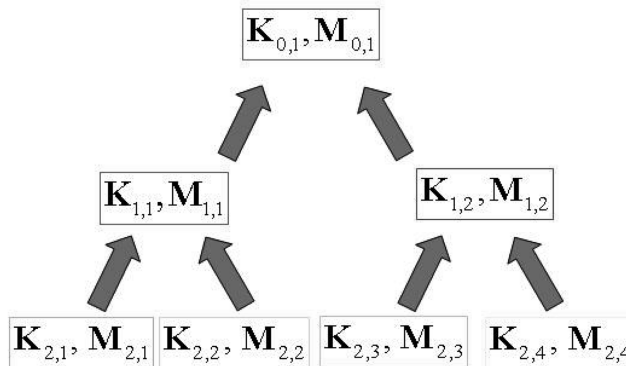


Fig. 2 Hierarchy of sub-structuring in the simple plate example

$$\bar{\mathbf{M}}^R = \mathbf{T}^T(\mathbf{U}^T\mathbf{M}\mathbf{U})\mathbf{T}$$

$$= \begin{bmatrix} \bar{\mathbf{M}}_{(2,1)}^R & 0 & \mathbf{T}_{(2,1)}^T \bar{\mathbf{M}}_{(2,1)(1,1)} \mathbf{T}_{(1,1)} & 0 & 0 & 0 & \mathbf{T}_{(2,1)}^T \bar{\mathbf{M}}_{(2,1)(0,1)} \mathbf{T}_{(0,1)} \\ & \bar{\mathbf{M}}_{(2,2)}^R & \mathbf{T}_{(2,2)}^T \bar{\mathbf{M}}_{(2,2)(1,1)} \mathbf{T}_{(1,1)} & 0 & 0 & 0 & \mathbf{T}_{(2,2)}^T \bar{\mathbf{M}}_{(2,2)(0,1)} \mathbf{T}_{(0,1)} \\ & & \bar{\mathbf{M}}_{(1,1)}^R & 0 & 0 & 0 & \mathbf{T}_{(1,1)}^T \bar{\mathbf{M}}_{(1,1)(0,1)} \mathbf{T}_{(0,1)} \\ & & & \bar{\mathbf{M}}_{(2,3)}^R & 0 & \mathbf{T}_{(2,3)}^T \bar{\mathbf{M}}_{(2,3)(1,2)} \mathbf{T}_{(1,2)} & \mathbf{T}_{(2,3)}^T \bar{\mathbf{M}}_{(2,3)(0,1)} \mathbf{T}_{(0,1)} \\ & & & & \bar{\mathbf{M}}_{(2,4)}^R & \mathbf{T}_{(2,4)}^T \bar{\mathbf{M}}_{(2,4)(1,2)} \mathbf{T}_{(1,2)} & \mathbf{T}_{(2,4)}^T \bar{\mathbf{M}}_{(2,4)(0,1)} \mathbf{T}_{(0,1)} \\ & & \text{symm.} & & & \bar{\mathbf{M}}_{(1,2)}^R & \mathbf{T}_{(1,2)}^T \bar{\mathbf{M}}_{(1,2)(0,1)} \mathbf{T}_{(0,1)} \\ & & & & & & \bar{\mathbf{M}}_{(0,1)}^R \end{bmatrix} \quad (12b)$$

$$\bar{\mathbf{x}}^p = [\mathbf{x}_{(2,1)}^p \ \mathbf{x}_{(2,2)}^p \ \mathbf{x}_{(1,1)}^p \ \mathbf{x}_{(2,3)}^p \ \mathbf{x}_{(2,4)}^p \ \mathbf{x}_{(1,2)}^p \ \mathbf{x}_{(0,1)}^p]^T \quad (12c)$$

2.2 The selection of the primary degrees of freedom

As mentioned in the introduction section, the selection scheme of PDOFs is very important in the system condensation method because it significantly influences accuracy of the reduced system. This paper employs the robust TLCS for the selection of PDOFs developed by Cho and Kim (2004) and the schematics of the TLCS is presented in Fig. 3.

In the first step, the reduced system is constructed through the estimation at the element-level using Rayleigh energy. In order to estimate the energy of each element, Ritz vectors need to be constructed as assumed modes through the Gram-Schmidt procedure as shown in Eq. (21).

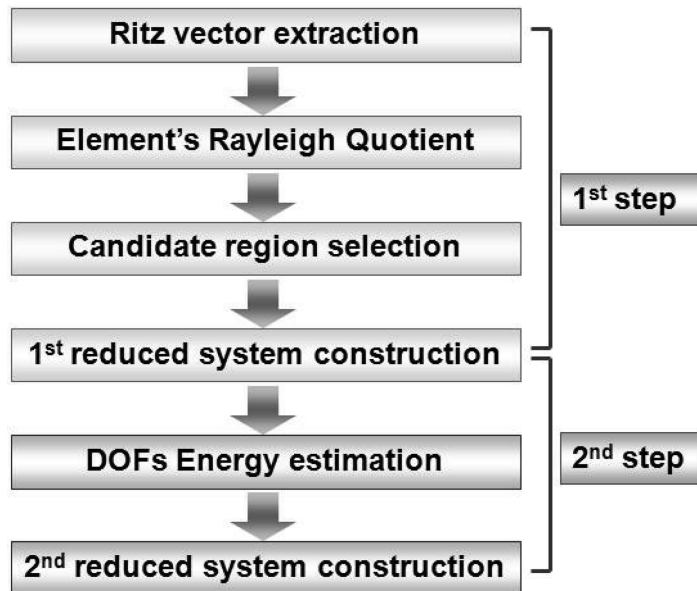


Fig. 3 Schematic configurations of the Two-Level Condensation Scheme (TLCS)

$$\mathbf{x}^{(i)} = \mathbf{x}^{(i)} - \sum_{k=1}^{i-1} \mathbf{x}^{(k)T} \mathbf{M} \mathbf{z}^{(k)}, \quad \mathbf{z}^{(k)} = \mathbf{x}^{(k)} / \sqrt{\mathbf{x}^{(k)T} \mathbf{M} \mathbf{x}^{(k)}} \quad (13)$$

After the sufficient number of Ritz vectors are obtained, the element-level energy estimator based on Rayleigh quotient can be obtained by summing the Rayleigh quotient calculated by each Ritz vector. The sum of the Rayleigh quotients of each i th element can be calculated as follows.

$$Ra_e^i = \sum_{k=1}^{NM} \frac{\mathbf{z}^{(k)T} \mathbf{K}_e^i \mathbf{z}^{(k)}}{\mathbf{z}^{(k)T} \mathbf{M}_e^i \mathbf{z}^{(k)}} \quad (14)$$

where NM is the number of Ritz vectors and $\mathbf{K}_e^i, \mathbf{M}_e^i$ are i th element stiffness and mass matrix, respectively. After estimating Rayleigh quotients for all the elements in the whole structure, the elements with the smaller first Rayleigh quotient are selected as primary elements. The first reduced system can be constructed through IRS technique, and the DOFs which are included in the primary elements are regarded as PDOFs.

In the second step, the final PDOFs are selected from the information of the reduced system which is constructed in the first step. In the previous TLCS, SEM is used as the DOF-wise selection scheme in the second step. However, Kim and Choi used the kinetic energy method (Kim and Choi 2000) instead of SEM. Because the reliability of TLCS is mostly determined in the first step, the difference between SEM and DOFs energy method is marginal in the basis on the solution accuracy. Even though accuracy between two methods is marginal, the kinetic energy method consumes smaller amount of computational resources than that of SEM. Through the second step, the final PDOFs can be selected. The TLCS is suitable to the interior parts of substructures because it is basically element-wise manipulation. However, systems of interface region between each substructure are constituted by the node-wised information. In this case, only the second step of TLCS is used for selection of PDOFs.

2.3 Time-frequency response analysis

Finally, the equation of equilibrium governing the linear dynamic response of a reduced system is presented as below.

$$\overline{\mathbf{M}}^R \ddot{\mathbf{x}}^p + \overline{\mathbf{C}}^R \dot{\mathbf{x}}^p + \overline{\mathbf{K}}^R \mathbf{x}^p = \overline{\mathbf{f}}^R(t) \quad (15)$$

where $\overline{\mathbf{K}}^R, \overline{\mathbf{C}}^R$ and $\overline{\mathbf{M}}^R$ is the final reduced stiffness, damping and mass matrices, and final damping matrix and applied force vector are also reduced to Eq. (16) which can be obtained similarly to the reduction procedure of stiffness and mass matrices.

$$\overline{\mathbf{C}}^R = \mathbf{T}^T (\mathbf{U}^T \mathbf{C} \mathbf{U}) \mathbf{T} \quad \text{and} \quad \overline{\mathbf{f}}^R(t) = \mathbf{T}^T \mathbf{U}^T \mathbf{f}(t) \quad (16)$$

Assuming a harmonic input, the applied force and displacement response vectors can be expressed as

$$\overline{\mathbf{x}}^R(t) = \mathbf{X}(\omega) e^{i\omega t} \quad \text{and} \quad \overline{\mathbf{f}}^R(t) = \mathbf{F}(\omega) e^{i\omega t} \quad (17)$$

The FRF of a structure can be evaluated using the displacement which is known as receptance (Ewins 1984).

$$\mathbf{D}(\omega) = \frac{\mathbf{X}(\omega)}{\mathbf{F}(\omega)} = (-\omega^2 \bar{\mathbf{M}}^R + j\omega \bar{\mathbf{C}}^R + \bar{\mathbf{K}}^R)^{-1} \quad (18)$$

The Newmark integration scheme is the one of the most popular methodologies for single step direct integration of 2nd order differential equation and it is widely used in many commercial codes. The Newmark method assumes a linear acceleration over the time interval as shown in Eq. (19). Moreover, the constant-average-acceleration method with $\theta = 0.5$ and $\gamma = 0.25$ is used for the stability of methodology (Bath 1996).

$$\begin{aligned} \dot{\bar{\mathbf{x}}}^p(t + \Delta t) &= \dot{\bar{\mathbf{x}}}^p(t) + (1 - \theta)\ddot{\bar{\mathbf{x}}}^p(t)\Delta t + \theta\ddot{\bar{\mathbf{x}}}^p(t + \Delta t)\Delta t \\ \bar{\mathbf{x}}^p(t + \Delta t) &= \bar{\mathbf{x}}^p(t) + \dot{\bar{\mathbf{x}}}^p(t)\Delta t + (0.5 - \gamma)\ddot{\bar{\mathbf{x}}}^p(t)\Delta t^2 + \gamma\ddot{\bar{\mathbf{x}}}^p(t + \Delta t)\Delta t^2 \end{aligned} \quad (19)$$

In this study, the Newmark time integration scheme is used for the transient time response analysis.

3. Numerical examples

In this section, the validity and applicability of the method are discussed by applying the algorithm to the example problems. Two structural models – a cantilever plate model and a wing-box model- are chosen for numerical demonstration. Two response – transient time response and frequency response – are studied to investigate accuracy with respect to the results of full system analysis. For the comparison, we reproduce the MBR method which is equivalent to methodology proposed Benninghof and Lehoucq (2004). Here, Ritz vectors used in TLCS technique is selected for the reduction of interior part of sub-structures as internal normal modes.

First example is a cantilever plate model of which numerical modeling is depicted in Fig. 4. This model is constituted by the four-node, hybrid shell element (Aminpour 1992) and the number of finite elements is 1896. The total number of DOFs is 11,724. This model is partitioned into four substructures through the two level graph partitioning process. A number of PDOFs is 371 which is 3.16% of original system.

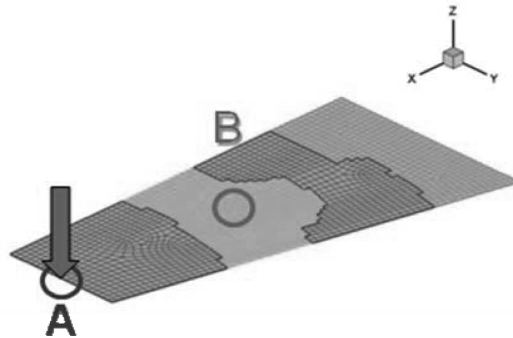


Fig. 4 Configuration of cantilever plate example

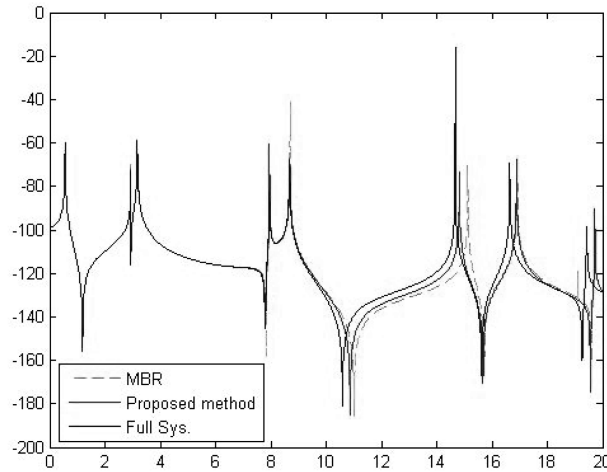


Fig. 5 The FRF graph (Receptance) of the cantilever plate example

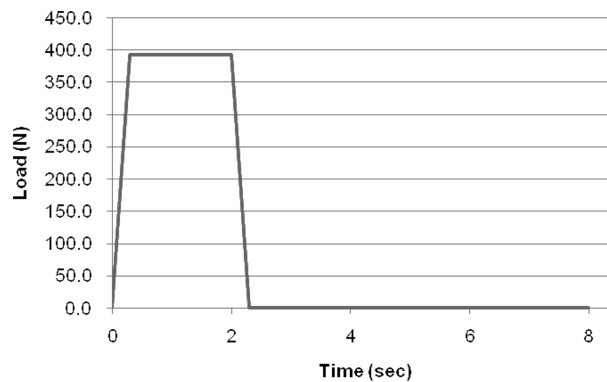


Fig. 6 An applied load profile of the cantilever plate example

Fig. 5 is the result of frequency response analysis of the cantilever plate. Loading position is the point A and displacement is computed at the point B as described in Fig. 4. In the frequency range from 0 Hz to 20 Hz, both methods - the proposed method and MRB - provides reliable solutions compared to the result of full system analysis as shown in Fig. 5. However, the proposed method can provide more accurate result than MRB in the frequency range from 10 Hz to 20 Hz. The accuracy of the proposed method shows the reliability of the present analysis.

The Newmark time integration scheme is conducted to get the transient time response. Here, we apply the step loading as shown in Fig. 6. Step loading whose magnitude is 400 N is applied during 2 seconds and the time response during 8 seconds is obtained. Time interval is 0.01 second and total time steps are 800, respectively. Displacement of point B which is in the transverse direction is plotted in Fig. 7. The errors of displacement between the propose method and the full system analysis are negligibly small.

Next, we illustrate the application of the proposed method to large-size FE system. Here, once more, the six DOF FE shell element which was used in the previous example is used. Wing-box

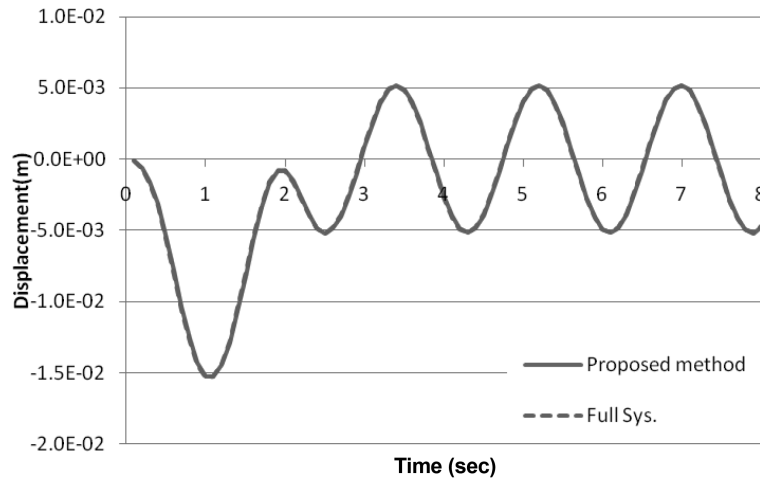
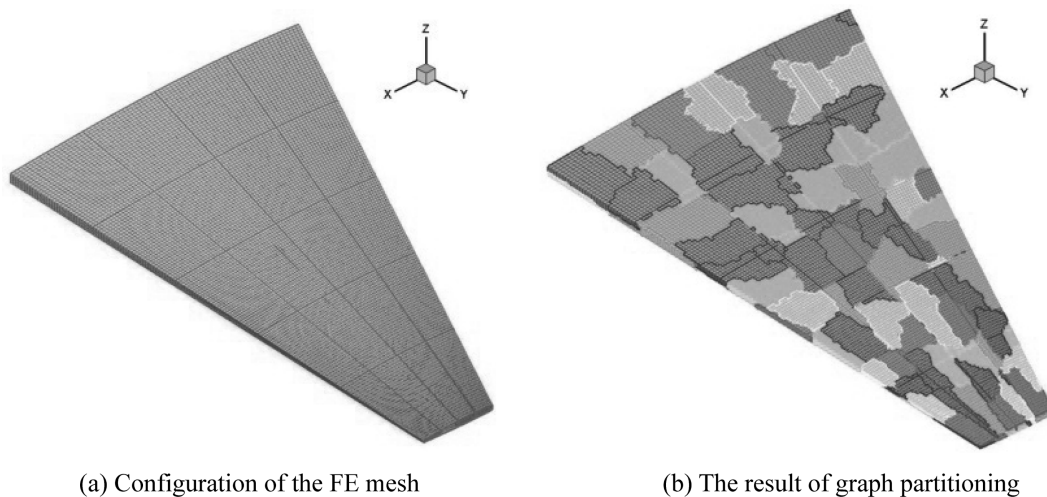


Fig. 7 Transient time responses of the cantilever plate example



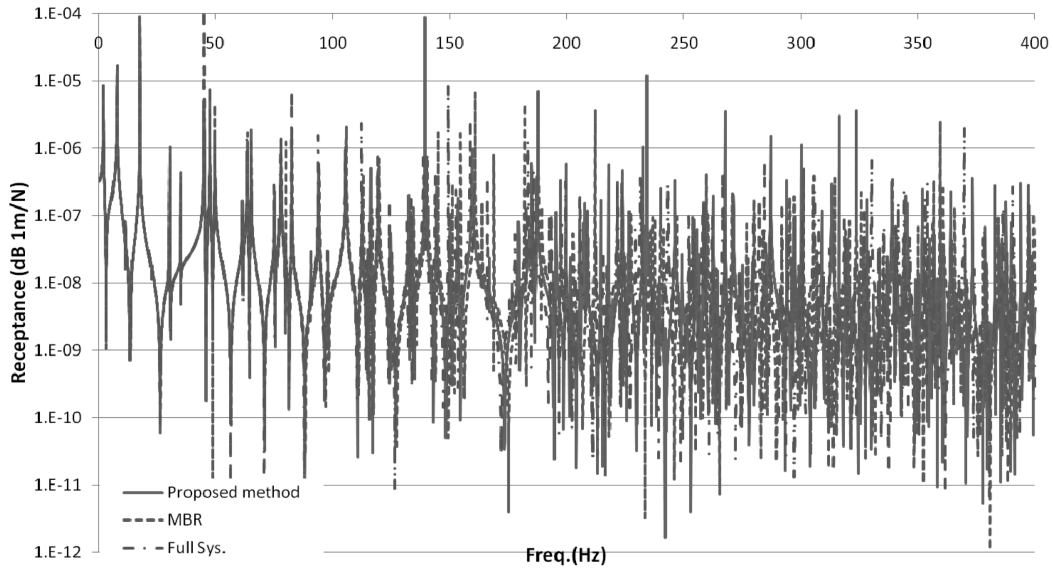
(a) Configuration of the FE mesh

(b) The result of graph partitioning

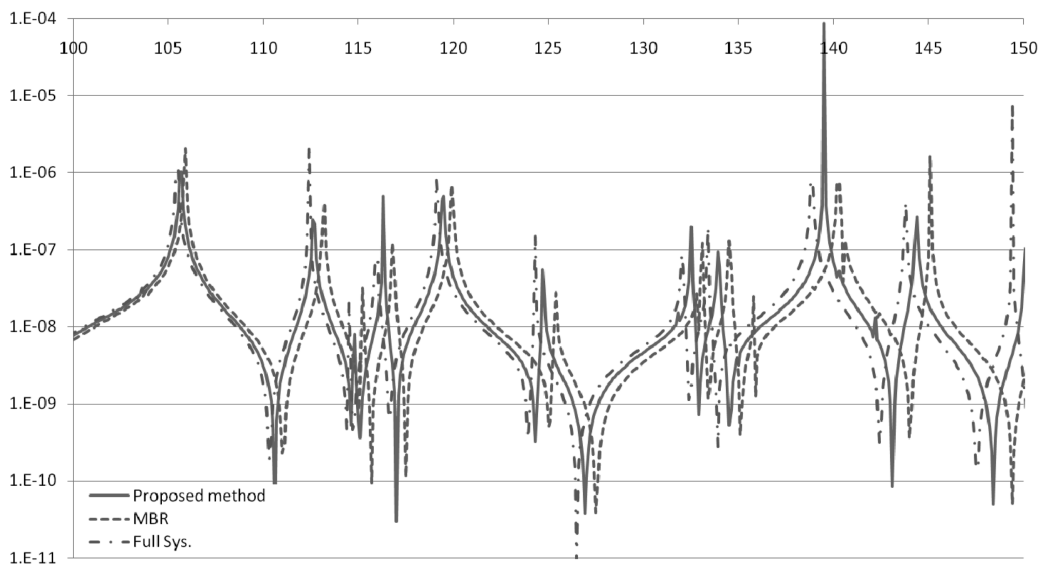
Fig. 8 Configurations for the wing-box example

model which is presented in Fig. 8(a) has 33,152 shell elements and 32,512 nodes. The total number of DOFs is 193k. This model is partitioned into 128 substructures through the seven level graph partitioning process as shown in Fig. 8(b). This model is reduced to the system which has PDOFs is 3,280, that is, size of reduced system is 1.69% to full system.

The result of frequency response analysis is up to 400 Hz frequency range and it is shown in Fig. 9(a). In the mid-range frequency (100~150 Hz), the MBR provides quite different results from the result of the proposed method as shown in the FRF result of Fig. 9(b). This trend is similar to that of the previous example. It should be mentioned that the proposed method needs only 17 minute for the entire calculation while the full system analysis requires more than 55 hour for the same calculation.



(a) the FRF graph(Receptance) in the overall frequency range until 400Hz



(b) the FRF graph(Receptance) in mid-frequency range from 100Hz to 150Hz

Fig. 9 The results of frequency response analysis of wing-box example

4. Conclusions

This study presents a combined method of TLCS, multi-level sub-structuring and IIRS to calculate a considerable number of eigenvalues for large-scale problems. First, the full system is partitioned by graph partition procedure. Next, the global system is decomposed using the block Gaussian

eliminator. From the decomposition, decoupled eigen-problems are approximated. Here, the PDOFs are selected by TLCs within every sub-eigen problem and IRS reduces whole decoupled eigen-problems into the reduced ones. Finally, the reduced system is constructed by the assembly of uncoupled reduced systems and eigen problem of assembled reduced system is solved through SIL method. The MLSC is applied to transient time response analysis and frequency response analysis.

The performance of the proposed method is verified by numerical examples. In comparison with the MBR, the proposed method shows remarkable improvement in the solution accuracy with preserving computational efficiency. The remarkable fact is that the proposed method has a significant advantage in both accuracy and efficiency as increment of system size. The proposed reduction method should serve as an efficient scheme in the analysis and design of large-scale structural dynamics problems. Non-linear problems and design optimization problems waits for their realizations.

Acknowledgements

This work was supported by the Korea Science and Engineering Foundation (KOSEF) through the National Research Lab. Program (No. ROA-2008-000-20109-0) and the WCU (World Class University) program (No. R31-2009-000-10083-0) funded by the Ministry of Science and Technology of Korea.

References

- Aminpour, M.A. (1992), "Direct formulation of a hybrid 4-node shell element with drilling degrees of freedom", *Int. J. Numer. Meth. Eng.*, **35**, 997-1013.
- Bath, K.J. (1996), *Finite Element Procedures*, Prentice Hall, USA.
- Bennighof, J.K. and Lehoucq, R.B. (2004), "An automated multilevel substructuring method for eigenspace computation in linear elastodynamics", *SIAM J. Sci. Comput.*, **25**(6), 2084-2106.
- Cho, M. and Kim, H. (2004), "Element-based node selection method for reduction of eigenvalue problem", *AIAA J.*, **42**(8), 1677-1684.
- Craig, Jr. R.R. and Bampton, M.C.C. (1960), "Coupling of substructures for dynamic analysis", *AIAA J.*, **6**(7), 1313-1319.
- Ewins, D.J. (1984), *Modal Testing: Theory and Practice*, Research Studies Press Ltd., England.
- Friswell, M.I., Garvey, S.D. and Penny, J.E.T. (1995), "Model reduction using dynamic and iterative IRS techniques", *J. Sound Vib.*, **186**(2), 311-323.
- Friswell, M.I., Garvey, S.D. and Penny, J.E.T. (1998), "The convergence of the iterated IRS method", *Earthq. Eng. Struct. D.*, **211**(1), 123-132.
- Guyan, R.J. (1965), "Reduction of stiffness and mass matrices", *AIAA J.*, **3**(2), 380.
- Henshell, R.D. and Ong, J.H. (1975), "Automatic masters from eigenvalues economization", *Earthq. Eng. Struct. D.*, **3**, 375-383.
- Hurty, W.C. (1968), "Vibration of structural systems by component mode synthesis", *J. Eng. Mech. Div.-ASCE*, **86**, 51-69.
- Kaplan, M.F. (2001), "Implementation of automated multilevel substructuring for frequency response analysis of structures", Ph.D. Dissertation, University of Texas at Austin.
- Kim, K.O. and Kang, M.K. (2001), "Convergence acceleration of iterative modal reduction methods", *AIAA J.*, **39**(1), 134-140.
- Kim, H. and Cho, M. (2006), "Two-level scheme for selection of primary degrees of freedom and semi-analytic

- sensitivity based on the reduced system”, *Comput. Meth. Appl. Mech. Eng.*, **195**, 4244-4268.
- Kim, H. and Cho, M. (2007), “Improvement of reduction method combined with sub-domain scheme in large scale problem”, *Int. J. Numer. Meth. Eng.*, **70**(2), 206-251.
- Kim, K.O. and Choi, Y.J. (2000), “Energy method for selection of degrees of freedom in condensation”, *AIAA J.*, **38**(7), 1253-1259.
- Lehoucq, R., Sorensen, D.C. and Yang, C. (1997), “ARPACK user’s guide: solution of large-scale eigenvalue problems with implicitly restarted arnoldi method”, SIAM, Philadelphia.
- O’callahan, J. (1989), “A procedure for an improved reduced system (IRS) model”, *Proceedings of 7th International Modal Analysis Conference*, 17-21.
- Shah, V.N. and Raymund, M. (1982), “Analytical selection of masters for the reduced eigenvalue problem”, *Int. J. Numer. Meth. Eng.*, **18**(1), 89-98.